

This article was downloaded by: [M. T. Hamed Mosavian]

On: 09 April 2013, At: 02:04

Publisher: Taylor & Francis

Informa Ltd Registered in England and Wales Registered Number: 1072954 Registered office: Mortimer House, 37-41 Mortimer Street, London W1T 3JH, UK



## Journal of Dispersion Science and Technology

Publication details, including instructions for authors and subscription information:

<http://www.tandfonline.com/loi/Idis20>

### Modeling of Oil-Water Emulsion Separation in Ultrasound Standing Wavefield by Neural Network

H. Ghafourian Nasiri<sup>a</sup>, M. T. Hamed Mosavian<sup>a</sup>, R. Kadkhodae<sup>b</sup> & J. Sargolzae<sup>a</sup>

<sup>a</sup> Department of Chemical Engineering, Faculty of Engineering, Ferdowsi University of Mashhad, Mashhad, Iran

<sup>b</sup> Department of Food Technology, Khorasan Institute of Food Research, Mashhad, Iran

Accepted author version posted online: 04 May 2012.

To cite this article: H. Ghafourian Nasiri, M. T. Hamed Mosavian, R. Kadkhodae & J. Sargolzae (2013): Modeling of Oil-Water Emulsion Separation in Ultrasound Standing Wavefield by Neural Network, Journal of Dispersion Science and Technology, 34:4, 490-495

To link to this article: <http://dx.doi.org/10.1080/01932691.2012.681997>

PLEASE SCROLL DOWN FOR ARTICLE

Full terms and conditions of use: <http://www.tandfonline.com/page/terms-and-conditions>

This article may be used for research, teaching, and private study purposes. Any substantial or systematic reproduction, redistribution, reselling, loan, sub-licensing, systematic supply, or distribution in any form to anyone is expressly forbidden.

The publisher does not give any warranty express or implied or make any representation that the contents will be complete or accurate or up to date. The accuracy of any instructions, formulae, and drug doses should be independently verified with primary sources. The publisher shall not be liable for any loss, actions, claims, proceedings, demand, or costs or damages whatsoever or howsoever caused arising directly or indirectly in connection with or arising out of the use of this material.

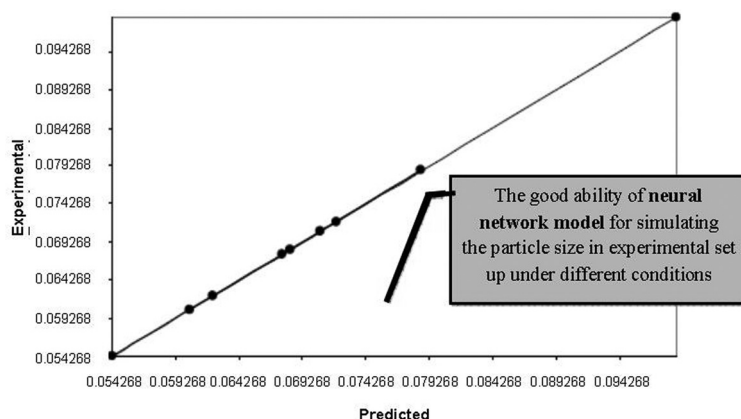
# Modeling of Oil-Water Emulsion Separation in Ultrasound Standing Wavefield by Neural Network

H. Ghafourian Nasiri,<sup>1</sup> M. T. Hamed Mosavian,<sup>1</sup> R. Kadkhodae,<sup>2</sup> and J. Sargolzae<sup>1</sup>

<sup>1</sup>Department of Chemical Engineering, Faculty of Engineering, Ferdowsi University of Mashhad, Mashhad, Iran

<sup>2</sup>Department of Food Technology, Khorasan Institute of Food Research, Mashhad, Iran

## GRAPHICAL ABSTRACT



A new approach has been introduced for separation of oil-in-water emulsion by using ultrasound standing wavefield. A neural networks model was used to simulate changes in the size of droplet during treatment. Model outputs were then validated and generalization capability was evaluated. For each network, the optimum values of isotropic spread were obtained by minimizing the root mean square error and maximizing the corresponding coefficient. It was found that the predicted values were in good agreements with experimental results. Also, increasing voice speed was demonstrated to predict size of emulsion particles more efficiently and accurately.

**Keywords** Neural networks, o/w emulsion, RBF, separation, ultrasound

## 1. INTRODUCTION

The amount of oily wastewater produced by different industries such as petrochemical, metallurgical, pharmaceutical, and food have been increasing every year causing environmental pollutions. Therefore, it is of necessary to employ a high efficient method in order to demulsified the mixture and to separate as much entrapped oil as possible.

Conventional technologies for breaking emulsion are centrifuge, chemical<sup>[1]</sup> and gravitational.<sup>[2,3]</sup> But demulsifi-

cation of very stable emulsions formed in industries containing fine droplets usually lead to achieve requiring energy and time. So other methods were used for emulsion separation such as thermal, electrical,<sup>[4,5]</sup> flotation and membrane.<sup>[6,7]</sup> But most of these conventional methods cannot efficiently remove micron or submicron sized oil droplets.<sup>[8–12]</sup> Hempoonsert used thermal demulsification of crude oil emulsion in water but this method could not be a proper technique for all emulsions as its thermal degradation effects and hard temperature control.<sup>[8]</sup> For chemical demulsification, demulsifier agent and its fraction must be known but it was depended on lots of parameters such as oil phase and its concentration in emulsion. Centrifuge separation was applied for small volume and as last step in separation process due to high consumption energy.<sup>[9]</sup>

Received 29 January 2012; accepted 5 March 2012.

Address correspondence to M. T. Hamed Mosavian, Department of Chemical Engineering, Faculty of Engineering, Ferdowsi University of Mashhad, Mashhad, Iran. E-mail: hmosavian@gmail.com or mosavian@um.ac.ir

Diaminger utilized membrane technology to break oil/water dispersions with several hydrophobic membranes and different modules, but separation efficiency was strongly proven to membrane fouling and initial oil concentration.<sup>[10]</sup> El-Kayar et al. developed an air flotation system in which chemical agents were used for further demulsification but the maximum amount of oil they could be removed was less than 50%.<sup>[11]</sup>

During the past few decades, the ability of low intensity ultrasonic standing wavefields to separate small particles from liquid suspensions has been widely used for different papers.<sup>[13,14]</sup> But only a few works have been reported oil/water emulsion separations.<sup>[15-17]</sup>

High intensity ultrasonic waves are usually used to prepare stable emulsions<sup>[18,19]</sup> or to measure emulsion creaming rate<sup>[20]</sup> but to author's best knowledge no attempt has been yet made to emulsion separation to its initial phases using high intensity ultrasonic standing wavefields.

This work was aimed at to investigate the feasibility and practicality of high intensity ultrasonic standing wavefield for breaking oil-in-water emulsion and separating the demulsified droplets. Another goal of this study was to use neural networks model to simulate changes in the size of droplets and check the effectiveness of the model and its generalization capability.

## 2. EXPERIMENTAL

### 2.1. Sample Preparation

Oil/water emulsions was prepared by homogenizing 5% sunflower oil in distilled water containing 2% Tween 80 as emulsifier using a rotor stator homogenizer (T 25 digital Ultra-Turrax, manufactured by IKA Laboratory) operating at 9000rpm for 3 minute. The coarse emulsion was further homogenized using a high intensity ultrasonic processor (VCX 750 Sonics) at a frequently of 20 kHz for 3 minutes at the maximum amplitude available. A titanium probe with face diameter of 19 mm, which was immersed 1 cm below the surface of sample was used for sonification. The temperature was kept constant at 25°C throughout by circulating cold water around the chamber. This procedure typically produced an emulsion with average droplet size ranging from 0.5 to 0.6  $\mu\text{m}$ .

### 2.2. Experimental Setup

The experiments were carried out in a rectangular open head chamber as shown in Figure 1.

It was (a double-walled) jacketed water bath with a depth of 9 cm. The ultrasound probe was screwed on one side of the chamber with the sample vessel immersed in water at different position relation to it. The distance between ultrasound source and reflector (left horizontal wall of chamber) was 48.5 cm.

The sample vessel was plexy glass with a dimension of 6  $\times$  2  $\times$  2 cm. The sample cell with 40 cc of prepared emul-

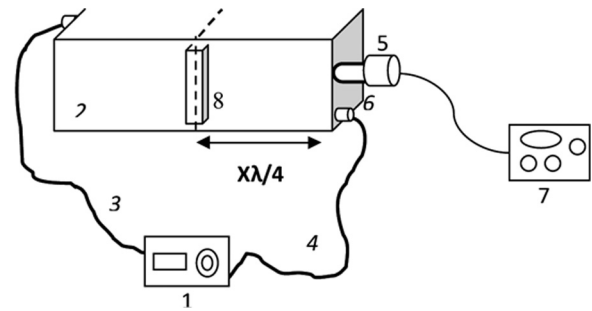


FIG. 1. Schematic of the acoustic chamber: 1) water bath; 2) chamber full with water; 3) water outlet; 4) water inlet; 5) transducer; 6) sound horn; 7) sonicator; 8) sample cell.

sion was immersed into the chamber at different distances from sound source. These positions were:  $7\lambda/4$ ,  $9\lambda/4$ ,  $11\lambda/4$ ,  $13\lambda/4$ ,  $15\lambda/4$ ,  $17\lambda/4$ ,  $19\lambda/4$ ,  $21\lambda/4$ , and  $23\lambda/4$  in which  $\lambda$  are wave length in pure water at 20°C. For every point, samples were irradiated for the period of 15, 30 and 45 minutes with the frequency of 20 kHz and input power (intensity) equal to 150 w. During irradiation time, temperature was kept constant in 20°C.

### 2.3. Measurements

Every experiment was carried out with three replications and results were averaged. At last, the experiments were characterized in terms of Souter diameter ( $d_{32}$ ) of treated emulsions using a Laser Particle Analyzer (Fritsch Analysette 22, Germany). This device calculated  $d_{32}$  from Lorenz-Mie model and Fraunhofer theory by relating scattering and breaking of laser light to droplet diameter. Emulsion samples were shaken before particle size measuring to have a uniform mixture of flocculated phase and water. The results are reported in Table 1.

## 3. STRUCTURE OF NEURAL NETWORK AND MODELING METHODS

### 3.1. Theory

The model proposed in this work is based on a radial basis function (RBF) network. Since the late-1980s, RBF networks have been a subject of study and have been employed with success in numerous fields,<sup>[21]</sup> their main applications being time series forecasting and function approximation. In general, it can be said that a RBF network is a feed forward network that consists of three layers: the input layer, the hidden layer and the output layer, as it is shown in Figure 2.

The hidden layer is composed of a determined number of nodes or basis functions. These basis functions, also called kernel, which can be selected among several types of functions, but for most applications they are chosen to be Gaussian functions. These types of functions have the

TABLE 1  
Experiment results

Distance from source ( $x\lambda/4$ )		0	7	9	11	13	15	17	19	21	23
$d_{32}(\mu\text{m})$	15 min	0.52	0.96	1.02	0.96	1.02	0.89	0.94	0.92	0.59	0.5
	30 min	0.52	1.1	1.31	1.32	1.18	1.08	1.12	0.98	0.85	1.15
	45 min	0.52	0.89	1.04	1.12	1.25	1.03	1.11	1.09	1.1	0.93

property of being local functions, which means that only they function with their centers close to the input patterns will give a response. So, the hidden layer is composed of a variable quantity of nodes, distributed over all the input space. Each node is a Gaussian function, characterized by a centre  $c$  and a width  $\sigma$  that produces a nonlinear output. Let's assume that the inputs of the network are given in a vector of  $d$  components,  $x = \{x_1, \dots, x_d\}$ , The activation function,  $g_j(x)$ , is of the form:

$$g_j(x) = \exp\left(-\frac{(x - c_j)^2}{\sigma_j^2}\right); \quad j = 1, 2, \dots, m \quad [1]$$

where  $c_j$  is the center of the activation function and  $\sigma_j$  its width.

In this research, the centers are set using the well known K-means algorithm.<sup>[22]</sup> The parameter  $m$  corresponds to the number of nodes in the hidden layer. The design and training of RBF networks consist of the number of hidden nodes and their structure which must be determined, that is, the centers and widths of the basis functions, and the weights of the output layer. There are several methods for constructing and training a RBF network,<sup>[23,24]</sup> and optimizing the design parameters,<sup>[25]</sup> but the most common case is that the number of basis functions has to be given by complex specifications or by means of a trial and error process. In this case, an own algorithm is implemented to select the structure and number of the basis functions using the optimization routines from Matlab.<sup>[26]</sup>

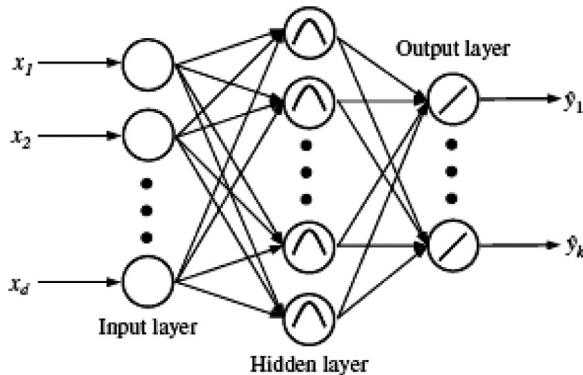


FIG. 2. RBF network structure.

### 3.2. Neural Network Design

This step consists of designing the radial basis layer (number of neurons, centers, and bias) as well as the calculus of the output layer weights. In order to do in theoretical part, many randomly selected patterns of each training test data (N 9 particle size) were used to design the net, constituting what it is called the training data set. The patterns corresponding to: maximum, minimum, and median values of input and output variables of each training test (N 21 particle size) employed to measure the net model accuracy, constituting what it is called the checking data set. The reason for limiting the training data in design of the neural network is, on one hand, to limit the time consumed in setting up the model and, on the other hand, to avoid unnecessary information that can cause over fitting. If all the data are included in a single neural network model, it is very difficult to obtain a converged result. Hence, the data set for device has been used in different models. The architecture of nets is different but the number of data is general for training and testing model.

Normalization of inputs leads to avoidance of numerical overflows due to very large or very small weights.<sup>[27]</sup> Therefore, data were normalized between the upper limit  $0 + \Delta_L$  and the lower limit  $1 - \Delta_U$ , where  $\Delta_L$  and  $\Delta_U$  are small margins used to give the network some extrapolation capability. The values for  $\Delta_L$  and  $\Delta_U$  used were 0.05.<sup>[28]</sup> Data were normalized using the linear normalization method as follows:

$$V_n = (1 - \Delta_U - \Delta_L) \frac{V - V_{\min}}{V_{\max} - V_{\min}} + \Delta_L \quad [2]$$

where  $V_n$  is the normalized value of  $V$ . The  $V_{\max}$  and  $V_{\min}$  are the minimum and maximum values of  $V$ , respectively,  $(1 - \Delta_U - \Delta_L)$  and  $\Delta_L$  are positive constants. The magnitudes of  $(1 - \Delta_U - \Delta_L)$  and  $\Delta_L$  should be in range of:  $\Delta_L \prec (1 - \Delta_U - \Delta_L) \prec 1$  and  $(1 - \Delta_U) \prec 1$ .

The performance of the neural network model evaluated using the root mean square error (RMSE). The determination coefficient ( $R^2$ ) of the modeled output and the measured training data can be related as follows:

$$R^2 = 1 - \frac{\sum_P (y_{\text{obs}} - y_{\text{est}})^2}{\sum_P (y_{\text{pred}} - \bar{y}_{\text{obs}})^2} \quad [3]$$

$$RMSE = \sqrt{\frac{\sum_P (y_{obs} - y_{est})^2}{N}} \quad [4]$$

$y_{obs}$ ,  $y_{est}$  are experimental and estimated values, respectively, and  $N$  is the number of data.

When the RMSE is at its minimum value and  $R^2$  is high,  $\geq 0.8$ , a model can be judged as very good.<sup>[29,30]</sup>

After this, the algorithm designs a group of neural networks using different spread values for the activation function in a wide range, from 0.01 to 100. Each of these neural networks, associated with a fixed spread, is designed with the training data set using the K-means algorithm increasing the number of neurons until the marginal prediction error is insignificant. The RMSE computed with the resulting neural network, nets, using the checking data is fixed as the goal for the next neural network design. The final stage of the algorithm consists of selecting the neural network as the one with minimum RMSE computed using the checking data set.

#### 4. RESULTS AND DISCUSSIONS

The output values of the model are classified into two groups. The first group shows the predicted values when using input patterns belonging to train the network, that is, near the training data set. These results allow checking the effectiveness of the model closer to the data set used for modeling. The second group represents the predicted values that do not belong to the training data set. These values will allow to validate the model. Figure 3 illustrates the best recall performances of RBF networks. As can be seen, all plots generated by RBF networks fit training data points.

For each network, the optimum values of isotropic spread were obtained by minimizing the root mean square error (RMSE) and maximizing determination coefficient ( $R^2$ ). Table 2 shows the RMSE and  $R^2$  results calculated, where different models with various spreads were used.

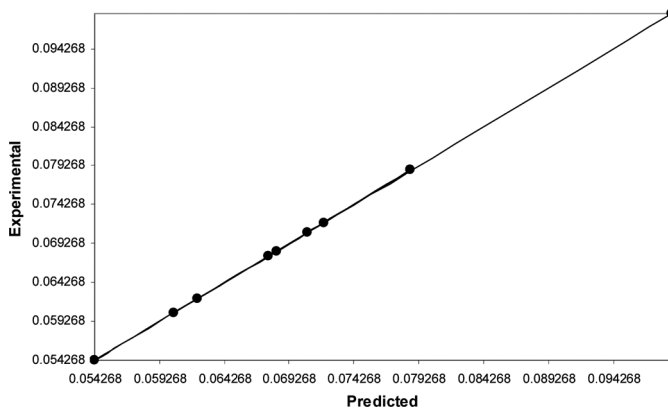


FIG. 3. Comparison between values of desired and the best RBF networks for all rotors with training data.

TABLE 2  
Root mean square error (RSME) and correlation coefficient ( $R^2$ ) for testing data in modeling with RBF network

Spread	Particle size ( $\mu\text{m}$ )	
	RMSE	$R^2$
0.01	0.001821	0.3635
0.9	0.002274	0.9906
<b>1</b>	<b>0.01054</b>	<b>0.9974</b>
1.2	0.02274	0.9906
5	0.0278	0.9931
10	0.01855	0.9913
100	0.01448	0.6444

It can be concluded that there would be an optimum model based on the test data. Since it provides the minimum degrees of freedom sustained by testing data points.

The corresponding generalization performance of these networks was small but unrealistic oscillations as shown in Figure 4.

Also in Figure 4, the results for experimental set up show a significant error compared to the other data. These fluctuations could be due to the noise content of the training data and might possibly be alleviated if the learning algorithm was equipped with some proper noise filtering facility (as in RBF networks).

Figure 4 presents a comparison between the experimental and predicted values for the set up used at optimum spread of RBF model. It can be seen that the predicted values for both groups, in term of minimum RMSE calculated from experimental data, are in a very good agreement with experimental data.

Examination of changes in the physical appearance of emulsion treated zones in relation to the ultrasound probe were revealed that some samples showed complete oiling off while in others signs of instability were observed. In last group; depending on range of changes; maximum three separate phase could be seen:

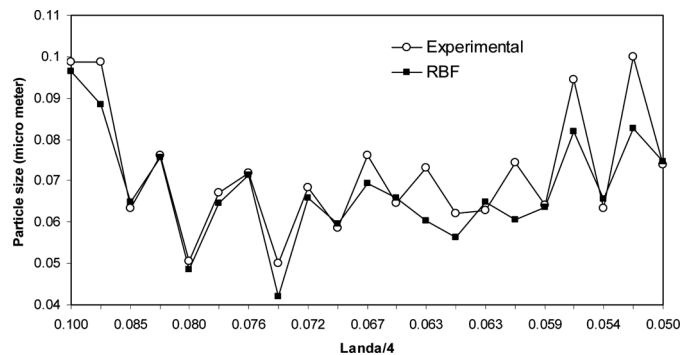


FIG. 4. Generalization performances of the best RBF networks for experimental data (set up) with testing data (S.D. = 0.0151).

1. bottom layer containing most of continuous phase and some stable oil droplet;
2. middle layer or cream which was lighter than the bottom one containing a compact amount of flocculated droplets; and
3. upper layer or oil phase.

But in most of samples only bottom and middle layers were formed depending on emulsion position in acoustic chamber. At  $11\lambda/4$  away from sound source, in addition to cream an oil layer also formed at the top. Oiling off was the last step in separation of oil from o/w emulsion. In that case system reached its maximum thermodynamic stability because oil-water interface descend to its minimum value.

Also as can be seen in Figure 4, over-fits in some points further increased by going away from the ultrasonic source. Ultrasound experimental system is depended on several factors such as sound intensity, cavitations forming, sound propagation, standing wave forming and position in ultrasound field that each one determined the state of experiment results.

Multiple scattering can occur by the bubbles cloud formed at the vicinity of the probe face with in the cavitations field. So; there is not a proper standing wave in that region due to formation of cavitation bubbles and the model can not foresee good value for such points.

Oil droplets must be pushed to antinode zone in a ultrasonic standing wavefield but in mentioned region no standing wave was formed.<sup>[15]</sup> The second reason for difference between experimental data and RBF analysis is due to low acoustic pressure in far area from sound source. In that case, energy level of sound wave is small, so the ability of ultrasound wave to bring oil droplets close together in emulsion decreases. The random nature of cavitation events could be another possible reason for the uncertainty observed.

The unregularized network clearly overfits the data at some data points and requires large oscillations to fit through (as shown in Figure 4). It can be seen that the predicted values are in good agreements with experimental results. Also, increasing voice speed led to the particle size improvement. For experimental set up, the maximum and minimum changes in the size of particles happened at acoustic source distance of  $11\lambda/4$  and  $23\lambda/4$ , respectively.

Therefore, an excellent agreement between experimental data and predicted values can be achieved by artificial neural networks and RBF model using the best isotropic spread.

#### 4. CONCLUSION

A novel method for separation of oil from oil/water emulsion has been developed. Separation efficiency due to coalescence and flocculation of droplets could be described by measuring changes in particle size.

In this research, the ability of neural network model was investigated for simulating the particle size of experimental set up in order to check the effectiveness of the model and its generalization capability under different parameters. For experimental set up, the maximum amount of droplet size happen at distance of  $11\lambda/4$  while sonicating at a distance of  $23\lambda/4$  lead to almost no changes in the size of droplets. Also it can be concluded that there is an optimum modeling using experimental data. Since it provides the minimum degrees of freedom sustained by testing data points. Also; corresponding generalization performance of these networks was small but unrealistic oscillations (Figure 4) and that the predicted values RBF model for both groups were in very good agreement with experimental data.

#### REFERENCES

- [1] Al-Sabagh, A.M., Maysour, N.E., and El-Din, M.R.N. (2007) *Journal of Dispersion Science and Technology*, 28 (4): 547–555.
- [2] Frising, T., Noik, C., and Dalmazzone, C. (2006) *Journal of Dispersion Science and Technology*, 7 (27): 1035–1057.
- [3] Fossen, M., Arntzen, R., Hemmingsen, P.V., Sjoblom, J., and Jakobsson, J. (2006) *Journal of Dispersion Science and Technology*, 27 (4): 453–461.
- [4] Less, S., Hannisdal, A., and Sjoblom, J. (2010) *Journal of Dispersion Science and Technology*, 31 (3): 265–272.
- [5] Less, S., Hannisdal, A., and Sjoblom, J. (2008) *Journal of Dispersion Science and Technology*, 29 (1): 106–114.
- [6] Bullon, J., Cardenas, A., and Sanchez, J. (2002) *Journal of Dispersion Science and Technology*, 23 (1): 269–277.
- [7] Shin, C. and Chase, G.G. (2006) *Journal of Dispersion Science and Technology*, 27 (4): 517–522.
- [8] Hempoonsert, J., Tansel, B., and Laha, S. (2010) *Colloids and Surfaces A*, 353: 37–42.
- [9] Gutiérrez, G., Lobo, A., and Allende, D. (2008) *Separation Science and Technology*, 43: 1884–1895.
- [10] Daiminger, D., Nitsch, W., Plucinski, P., and Hoffmann, S. (1995) *Membrane Science*, 99: 197–203.
- [11] El-Kayar, A., Hussein, M., Zatout, A.A., Hosny, A.Y., and Amer, A.A. (1993) *Separation Technology*, 3: 25–31.
- [12] Honga, A., Fane, A.G., and Burford, R. (2003) *Journal of Membrane Science*, 222: 19–39.
- [13] Martin, S.P. and Townsend, R.J. (2005) *Biosensors and Bioelectronics*, 21: 758–767.
- [14] Haake, A. and Dual, J. (2002) *Ultrasonics*, 40: 317–322.
- [15] Nii, S., Kikumoto, S., and Tokuyama, H. (2009) *Ultrasonics Sonochemistry*, 16: 145–149.
- [16] Ye, G. and Lu, X. (2008) *Chemical Engineering and Processing*, 47: 2346–2350.
- [17] Stack, L.J. and Carney, P.A. (2005) *Ultrasonics Sonochemistry*, 12: 153–160.
- [18] Canselier, J.P., Delmas, H., Wilhelm, A.M., and Abismail, B. (2002) *Journal of Dispersion Science and Technology*, 23 (1): 333–349.
- [19] Mosavian, M.T.H. and Hassani, A. (2010) *Journal of Dispersion Science and Technology*, 31(3): 293–298.
- [20] Howe, A.M., Mackie, A.R., and Robins, M.M. (1986) *Journal of Dispersion Science and Technology*, 7(2): 231–243.

- [21] Bishop, C.M. (1994) *Review of Scientific Instruments*, 65: 1803–1832.
- [22] MacQueen, J. (1967). Some methods for classification and analysis of multivariate observations. In *Proceedings of the Fifth Symposium on Mathematical Statistics and Probability*. Berkeley, CA: University of California Press.
- [23] Billings, S.A. and Zheng, G.L. (1995) *Journal of Neural Networks*, 8: 877–890.
- [24] Sarimveis, H., Alexandridis, A., Tsekouras, G., and Bafas, G.A. (2002) *Industrial & Engineering Chemistry Research*, 41: 751–759.
- [25] de Lacerda, E.G.M., Ludernier, T.B., and de Carvalho, A.C.P.L.F. (2000) 6th Brazilian Symposium on Neural Networks, Brazil, November 22–25.
- [26] Matlab R14 SP2. 2005, Mathworks Inc.
- [27] Menhaj, M.B. (1998) *Fundamentals of Neural Networks*, Professor Hesabi Publishers. (in Persian)
- [28] Sargolzaei, J. (2006) *Modeling and Simulation of Milk Ultrafiltration Process Using Adaptive Neuro-Fuzzy Inference Systems*, Department of Chemical Engineering, University of Sistan & Baluchestan.
- [29] Sargolzaei, J., Saghatroleslami, N., Khoshnoodi, M., and Mosavi, M. (2006) *J. Chem. Chem. Eng.*, 25: 67–76.
- [30] Kasabov, N.K. (1998) *Foundations of Neural Networks, Fuzzy Systems and Knowledge Engineering*; Cambridge, MA: MIT Press.